Advances in Sample Preparation 20 (2026) 100249

Contents lists available at ScienceDirect

Advances in Sample Preparation

journal homepage: www.elsevier.com/locate/sampre

# Nasal exudate sampling for GFAP determination: A comparative study of collection devices and recovery methods for point-of-care stroke diagnosis

Pablo Rioboó-Legaspi [a], Estefanía Costa-Rama [a,b,*], Beatriz Fernández [a,b], Carmen García-Cabo [c,d], Lorena Fernández-Benavente [c,d], Sergio Calleja-Puerta [c,d], M. Teresa Fernández-Abedul [a,b,*]

[a] Department of Physical and Analytical Chemistry, Universidad de Oviedo, Oviedo, Spain
[b] Biomedical Engineering Centre, Universidad de Oviedo, Oviedo, Spain
[c] Neurology Department, Hospital Universitario Central de Asturias, Oviedo, Spain
[d] Clinical and Basic Neurology Research Group, Instituto de Salud del Principado de Asturias (ISPA), Oviedo, Spain

ARTICLE INFO

*Keywords:*
Nasal exudate
Nasal sampling
Biomarkers
Glial fibrillary acidic protein
Swabs

ABSTRACT

The discovery of a brain-nose discharge through the glymphatic clearance pathway across the cribriform plate has opened new possibilities for biomarker-based diagnostics of neurological disorders. Glial fibrillary acidic protein (GFAP) is a clinically relevant biomarker for early differentiation between hemorrhagic and ischemic stroke, yet its low abundance in nasal exudate (NE) poses significant analytical challenges. Current nasal sampling devices and processing workflows are commonly aimed at infectious respiratory diseases, where analyte concentrations are substantially higher. In this study, three NE collection devices (flocked nylon swabs, GrooveSwab®, and Nasosorption™ swabs) have been evaluated alongside multiple recovery protocols for their effectiveness in recovering GFAP from NE. Flocked nylon swabs demonstrated superior protein recovery and patient comfort, making them the most appropriate option for GFAP determination. In contrast, although GrooveSwab® and Nasosorption™ swabs exhibited lower protein recovery, they showed potential for applications involving higher analyte concentrations or alternative diagnostic formats. Recovery protocols combining vortexing and centrifugation provided the highest GFAP release with minimal losses. Overall, these findings support the feasibility of decentralized NE sampling for GFAP determination and highlight its potential integration into rapid, minimally invasive point-of-care workflows for stroke diagnosis.

## Introduction

Within the field of neurology, rapid and accurate diagnostics are essential for obtaining rapid, cost-effective, and decentralized information to guide early clinical decisions and improve patient outcomes. This is particularly critical in the case of stroke, where a delay in the diagnosis and classification of the type of stroke (ischemic vs. hemorrhagic) directly influences morbidity and mortality. Currently, stroke diagnosis still relies heavily on clinical criteria and neuroimaging techniques, such as magnetic resonance imaging (MRI), computed tomography (CT), or positron emitting tomography (PET) scans. While mobile stroke units (MSUs) have the potential to decentralize these technologies [1], they remain expensive and require specialized personnel. Thus, biomarker-based diagnostics would represent a significant advancement in the management of neurological conditions such as stroke [2]. Although numerous biomarkers have been identified for stroke diagnosis, their integration into clinical practice remains limited [3].

Among the biomarkers proposed for stroke diagnosis, glial fibrillary acidic protein (GFAP) has emerged as one of the most promising candidates for distinguishing hemorrhagic from ischemic stroke within the first hours after symptoms onset [4–6]. GFAP is an astrocytic protein released into biological fluids following intracerebral hemorrhage, and its early elevation has been widely reported in blood and cerebrospinal fluid (CSF) [4,7]. Because emergency stroke care requires diagnostic tools that can be deployed rapidly and without specialized infrastructure, GFAP constitutes an appropriate model CNS biomarker for evaluating alternative sampling strategies aimed at decentralized stroke triage.

When studying biomarkers from the central nervous system (CNS), the presence of the blood-brain barrier (BBB) limits the transfer of many

* Corresponding authors.
*E-mail addresses:* costaestefania@uniovi.es (E. Costa-Rama), mtfernandeza@uniovi.es (M.T. Fernández-Abedul).

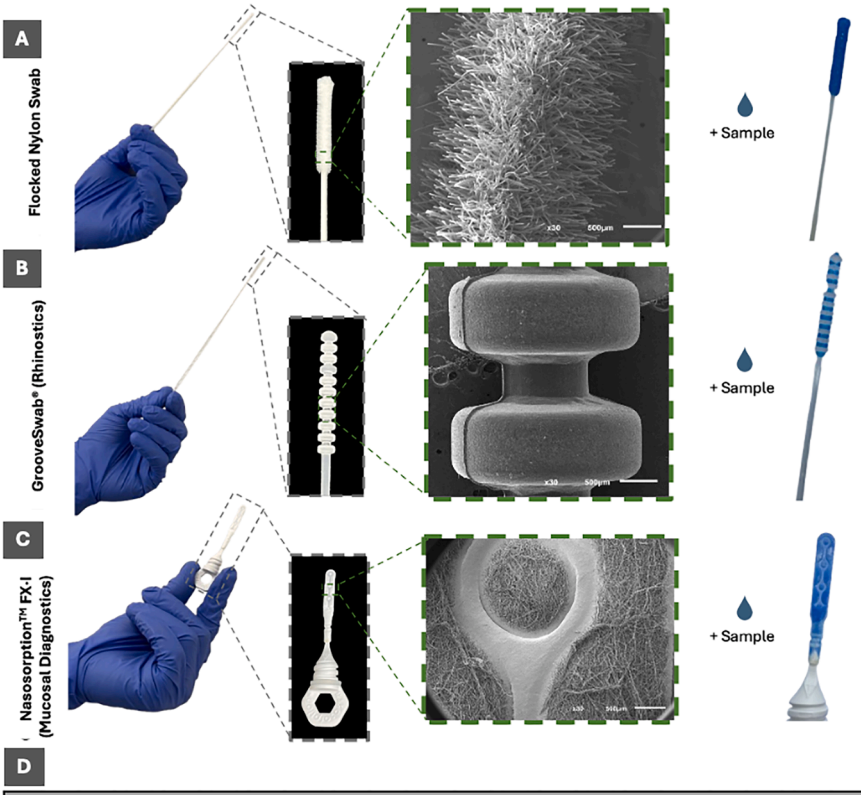
https://doi.org/10.1016/j.sampre.2026.100249
Received 22 May 2026; Received in revised form 3 September 2026; Accepted 16 September 2026
Available online 6 October 2026
2772-5820/© 2026 Published by Elsevier B.V. This is an open access article under the CC BY-NC-ND license (http://creativecommons.org/licenses/by-nc-nd/4.0/).

CNS-derived proteins to peripheral blood. Thus, biomarkers have been most studied through CSF *via* lumbar puncture, a highly invasive procedure. However, recent advances have focused on collecting CNS information through nasal exudate (NE) due to the olfactory region's proximity to the brain through the cribriform plate, with a porosity that enables the discharge of fluids from the brain's glymphatic system into the nasal cavity. This brain-clearance pathway has been extensively studied in both animal and human models, offering a promising, non-invasive approach to obtain brain-related information from a region anatomically closer to the CNS than conventional peripheral sample sources [8]. For instance, β-amyloid proteins have been detected in the nasal discharge of Alzheimer's patients [9,10], while differential levels of iron [11,12], GFAP [13], ferritin and ferroportin [14] have been found in ischemic and intracerebral hemorrhage stroke patients' nasal exudate. These findings suggest that NE may offer a non-invasive and anatomically proximal window into CNS pathology, with potential applicability to emergency diagnostics.

Traditionally, methods for sampling fluids from the nasal cavity have focused on the diagnosis of respiratory infections, and most collection devices and protocols have been developed with this purpose in mind [15]. The COVID-19 pandemic spurred the creation of many new nasal sampling devices, but their suitability for recovering low-abundance proteins, such as GFAP, remains insufficiently characterized.

In the field of nasal sampling, swab-based devices remain the most widely used tools. These differ mainly in three aspects: i) the shaft material, typically polymeric, though metallic variants exist; ii) the collection tip, which may be cellulosic (e.g., cotton), or synthetic (e.g., nylon); and iii) the configuration of the collection material, defined by the geometry of the tip (cylindrical, planar, etc.) and the attachment method (woven, flocked, pressed, etc.).

Within this, flocked nylon swabs have become the most relevant player. These devices are made of a plastic shaft, pre-treated for the electrostatic flocking of thousands of perpendicular nylon fibers, forming a brush-like structure (Fig. 1A) [16]. This unique structure leads to enhanced capillary action and release efficiency when compared to woven swabs, as traditional cotton swabs may trap sample components




D

| Device | | Flocked Nylon Swab | GrooveSwab® | Nasosorption™ FX-I |
|---|---|---|---|---|
| **Material** | | Nylon | Polypropylene | SAM™ |
| **Absorption method** | | Capillarity | Surface Tension | Capillarity |
| **Total length (mm)** | | 150 | 150 | 60 |
| **Collection part size (mm)** | length | 20 | 20 | 27 |
| | width | 3 | 2.5 | 4.5 |
| | thickness | 3 | 2.5 | 2 |
| **Collected aqueous solution (mg)** | | 80 ± 11 (14%) | 11 ± 2 (18%) | 70 ± 15 (21%) |
| **Collected NE sample (mg)** | | 30 ± 12 (40%) | 8 ± 4 (50%) | 40 ± 18 (45%) |
| **Patient comfort ranking** | | 1st (n=14) | 2nd (n=14) | 3rd (n=14) |

SAM™:Synthetic absorptive matrix
NE: Nasal exudate

**Fig. 1.** Devices used in this study and its characteristics. A: Flocked nylon swab, B: GrooveSwab®, and C: Nasosorption™. Left: Pictures of the device for real size comparison, with details of the tip of the device (grey) and SEM images of the collection part (green). Right: Picture of the device after being immersed in a 0.001% solution of MB in water. D: Summary of the characteristics of the devices. Collected liquid and sample are given in terms of mean ± SD. RSDs (in %) are given between brackets (n = 10 unless otherwise stated).

within the tightly woven fibers [17]. Flocked swabs are usually more patient friendly, when compared to swabs with a shaft made of other materials (wood, steel, etc.) or other nasal sampling techniques such as nasal washing, as the flexible shaft and soft fibers lead to less discomfort, which is a key factor when sampling sensitive areas, such as the nasal cavity.

As mentioned before, the COVID-19 pandemic accelerated the development of alternative nasal sampling devices with alternative collection principles. In this aspect, two more devices have been considered in this study: GrooveSwab® (Rhinostics Inc.), which consists of a plastic shaft with a honey dipper-like series of plastic discs which collect the sample by surface tension (Fig. 1B), and Nasosorption™ FX·I (Mucosal Diagnostics), which incorporates a synthetic absorptive matrix (SAM™) that captures fluid by capillarity [18] (Fig. 1C). The latter features a rigid, hot-pressed fiber pattern designed to improve handling and structural stability.

In this study, these three commercially available tools for NE collection were evaluated for the recovery of GFAP, used here as a model CNS biomarker due to its clinical relevance in emergency stroke diagnosis, from simulated and real NE samples. Different sample-processing workflows are compared, assessing volumetric and protein recovery, and discussing the implications of device design and handling on analytical performance. The aim of this work is to determine which sampling strategies are most suitable for recovering low-abundance proteins from NE, with a specific focus on their potential application in rapid, minimally invasive differential stroke diagnosis.

## Methods

### *Sampling devices*

Three devices were used in this study: Flocked nylon swabs, purchased from Biocomma (SW01E); Nasosorption™ FX·I (shortened as Nasosorption™), purchased from Mucosal Diagnostics; and GrooveSwab®, provided by Rhinostics Inc.

### *General material and reagents*

Phosphate buffered saline (PBS) tablets, methylene blue (MB) and bovine serum albumin (BSA) were purchased from Sigma-Aldrich. Milli-Q® water was purified using a Direct-Q UV system. COVID tests were purchased from Boson Biotech (Rapid SARS-CoV-2 Antigen Test Card, 1N40C5). Scanning electron microscopy (SEM) images of the devices were obtained with a JSM 6610LV from JEOL.

### *Immunoassay for GFAP determination*

GFAP concentration was quantified using a spectrophotometric immunoassay based on a modified protocol of a commercial antibody-pair kit previously reported [13]. The antibody pair (including the GFAP standard), 96-well microplate, and streptavidin-horseradish peroxidase (HRP) were obtained from Abcam (ab222279, ab210903, ab210901, respectively). The assay workflow is summarized below.

Each well was first coated with 50 μL of a 2 μg/mL capture antibody solution prepared in coating buffer (CB; 35 mM $NaHCO_3$, 15 mM $Na_2CO_3$, pH 9.6) and incubated for 2 h. After washing with washing buffer (WB; 1 × PBS, 0.05% Tween® 20, pH 7.3), plates were blocked overnight at 4 °C using blocking buffer (BB; 1 × PBS, 0.05% Tween® 20, 1% BSA, pH 7.3). The following day, plates were washed and 50 μL of GFAP standards (in BB) or sample solutions were added and incubated for 2 h. After washing, 50 μL of a 2 μg/mL detection antibody solution in BB were added and incubated for 1 h. Plates were washed again and incubated for 1 h with 50 μL of streptavidin-HRP (0.05 μg/mL in BB). Following a final wash, 100 μL of 3,3′,5,5′-tetramethylbenzidine (TMB) substrate were added and allowed to react for 30 min protected from light. The reaction was stopped with 100 μL of 1 M $H_2SO_4$, and absorbance was recorded at 450 nm using an Eon™ microplate reader (BioTek). All steps were performed at room temperature with shaking at 400 rpm unless otherwise specified. Washing steps consisted of three cycles with WB. Each assay included its corresponding calibration curve using increasing GFAP concentrations (pg/mL). An example of a calibration curve is provided in Fig. S1 of the Supplementary Material.

### *Protocols for sample processing*

The recovery buffer consisted of 10 mM (i.e., 1 x) PBS pH 7.4 supplemented with 1% of BSA. Simulated samples were prepared by diluting GFAP standards in the same buffer. Depending on the device, samples were either loaded by dipping the collection material into the simulated solution for 10 s, or by depositing a defined volume directly onto the device.

Unless otherwise stated, each device was immediately transferred to an appropriate storage tube (15 mL Protein LoBind® Tubes, Eppendorf for flocked nylon swab and GrooveSwab®, and the manufacturer-provided tube for Nasosorption™) after collecting the simulated sample and stored at −80 °C until being processed. Sample recovery was then performed following one of the protocols described below:

- Manual mixing (A): the device tip or absorbent part was placed in 200 μL (flocked nylon swabs, GrooveSwab®) or 1 mL (Nasosorption™) of the recovery buffer and manually twisted at a constant speed for 1 min.
- Vortex mixing (B): the device tip or absorbent part was placed in 200 μL (flocked nylon swabs, GrooveSwab®) or 1 mL (Nasosorption™) of the recovery buffer and the shaft was carefully cut. After that, the tube with the device was mixed in a vortex for 2 min total, in 10 s intervals with 10 s rest intervals.
- Vortex mixing plus centrifuging (C): After vortex mixing, devices were transferred to a centrifuge spin column (Labbox SPIN-DNG-10; filtration membrane removed) and centrifuged at 16,000 x g for 5 min.
- Buffer-free centrifuging (D): Device tips were cut and placed directly into the spin column to thaw, followed by centrifugation at 16,000 x g for 5 min.
- Buffer-free centrifuging (No freezing, E): Same as the previous protocol, but devices were processed immediately without prior storage at −80 °C.

All the steps were performed in Protein LoBind® tubes, except for those steps involving centrifugation, in which case the eluate was collected in the spin-column tube. To assess potential GFAP losses associated with the tubes and spin columns, a control experiment was performed in the absence of any collection device. For this, 20 μL of recovery buffer solutions containing different GFAP concentrations were placed in Protein LoBind® tubes and either processed immediately or stored at −80 °C before thawing and processing. In both cases, samples were transferred to membrane-free centrifuge spin columns and centrifuged at 16,000 x g for 5 min, following the same conditions used in the device-processing protocols. GFAP was subsequently quantified using the immunoassay described above.

### *Calculation of volume and protein recovery*

Volume recoveries were calculated gravimetrically. For each protocol, the collection vessel (microcentrifuge tube or spin column) was weighed before and after the elution step. The difference in mass was converted to volume considering the solution density (1.012 g/mL, determined prior to the experiments). In buffer-containing protocols, the recovered volume corresponds to the difference between the eluted mixture (buffer and released sample) and the buffer volume used. In buffer-free protocols, the measured mass directly reflects the volume of sample recovered from the device. Volumetric recovery (%) was calcu-

lated as the ratio between the recovered volume and the initial volume applied to the device:

$$Volumetric\ recovery\ (\%) = 100\ \times\ \frac{Recovered\ volume\ (mL)}{Collected\ volume(mL)}$$

These measurements were only performed for protocols involving centrifugation, where the device was fully removed from the solution, allowing accurate gravimetric determination.

Protein recovery was estimated as 100 times slope of the regression obtained between expected and measured GFAP concentrations, which represents an average recovery across the tested range. The regression included the (0,0) point because this data corresponds to the analyte blank (0 pg/mL GFAP), whose absorbance intensity was set to zero. This reflects the expected zero-signal condition in the absence of analyte.

### *Sample analysis*

The research was conducted according to the Declaration of Helsinki ethical principles for medical research involving humans. All subjects have signed the written informed consent, and the study protocol was reviewed and approved by the Ethics Committee of the Principality of Asturias (approval number 198/16). NE samples from 10 healthy volunteers were collected using all 3 devices. In the case of stroke patient samples, NE samples were obtained from 4 consecutive stroke patients who were admitted to the Stroke Unit of the HUCA and were over 18 years of age. Patients with nosebleeds or refusal to sign informed consent were excluded from the study. NE samples were obtained within 48 h from the symptoms onset, using the three devices in a random order for each patient. Collection devices were weighed before and after sampling using a 5-digit analytical balance (LA 124i, VWR) to determine the collected mass.

For assessing the feasibility of Nasosorption™ swabs in SARS-CoV-2 lateral flow immunoassays (LFIA), nasopharyngeal swab samples were collected at HUCA. Swabs were placed in 1.5 mL tubes containing 500 μL of 10 mM Tris-EDTA buffer solution (TE, pH 8.0). Samples were heated at 95 °C during 5 min prior to its transportation [15] for extrahospital analysis. qPCR results for validation purposes were provided by the Service of Microbiology of the HUCA.

### *Application of Nasosorption™ to lateral flow immunoassays*

To evaluate the integration of Nasosorption™ swabs with lateral flow immunoassays (LFIAs), devices were prepared by depositing 20 μL of previously extracted nasal swab samples, and left to dry at room temperature for 5 min. Then, the LFIA cassette was opened, and the Nasosorption™ swab was placed over the sample pad before closing the housing. After that, 4 drops of the buffer solution supplied with the LFIA were dropped on the sample pad. Pictures were then subsequently taken after 15 min.

### *Statistical analysis*

Statistical analyses were performed using two-tailed Student's t-tests, applied to pairwise comparisons after verifying the underlying assumptions of normality (Shapiro–Wilk test) and homoscedasticity (Levene's test). A significance threshold of $p < 0.05$ was used throughout, and results are reported as mean ± SD (Standard Deviation) unless otherwise stated.

## Results

### *Comparison of nasal exudate collection devices*

Prior to any characterization of their performance in the determination of proteins, we first examined the morphological and physical properties of the three nasal exudate collection devices. SEM imaging (Figs. 1A-C; additional surface details in Fig. S2) revealed distinct structural features that directly influence fluid uptake and release. To assess absorption capacity, each device was tested using a 0.001% methylene blue solution in water, dipping the device into this solution (used as simulated sample) for 10 s. The collected masses are summarized in Fig. 1D. Additionally, real NE samples from healthy volunteers were also collected and weighed. In the case of the flocked nylon swabs, a significant difference was observed between simulated and real samples (≈ 50 mg, $p = 1.2{\cdot}10^{-7}$), with Nasosorption™ swabs showing a similar trend (≈ 30 mg, $p = 2.4{\cdot}10^{-4}$). In contrast, GrooveSwab® displayed minimal variation (≈ 3 mg, $p = 0.1$). These differences align with the size of the device and the collection mechanisms, as the thin surface tension-driven discs of the GrooveSwab® saturate with a small amount of sample, whereas capillary-driven devices can theoretically absorb larger volumes than those typically obtained from real NE samples. It is also important to note that, when working with real NE samples, the amount of sample mass collected is highly variable, as reflected by the high relative standard deviations (RSD) observed. This variability underscores the need for standardized procedures, not only for sample recovery but also for reference markers, since it is currently essential to weigh each device before and after sampling to accurately determine the mass of sample absorbed. This step becomes particularly critical when dealing with low-abundance biomarkers, as even small differences in collected mass can substantially affect the final measured concentration.

User comfort was evaluated in 10 healthy volunteers and 4 stroke patients, who ranked the devices from most to least comfortable, after sequential sampling. Device order was randomized to avoid bias. As shown in Fig. 1D, flocked nylon swabs were consistently rated as the most comfortable, with 100% of the participants ranking them first. GrooveSwab® and Nasosorption™ were ranked second and third, respectively, with 71% preferring GrooveSwab® over Nasosorption™ (with only 29% ranking it as the second most comfortable choice). All stroke patients provided identical rankings. These differences in comfort can be explained not only by the material stiffness and size of the device, but also by the collection protocol, as both the nylon flocked swab and the GrooveSwab® rely on inserting the swab into the nostril and collecting the sample with circular movements, while the Nasosorption™ collection protocol involves introducing and pressing the device into each nostril for 1 min.

### *Recovery analysis using different processing protocols*

To study the efficiency of these devices in GFAP collection and recovery, an initial study was carried out with flocked nylon swabs, given their widespread use in clinical and analytical sampling. Numerous studies have characterized their performance for sampling and recovery of DNA [19,20], whole microorganisms [16,21], bacterial spores [22] and viral particles [23], supporting their suitability as a reference tool. This preliminary assay (Fig. 2A grey, pink and green protocols in the flowchart) consisted of collecting a simulated sample (10 mM PBS buffer containing 1% BSA and a known concentration of GFAP) by dipping the swab into 1 mL of this solution. The swab was then transferred to an empty collection tube and subsequently frozen at −80 °C prior to analysis.

For this purpose, the swab was transferred into 200 μL of 10 mM PBS solution to thaw. After that, 3 sample processing protocols were evaluated (Fig. 2A, see Methods section): manual mixing (A); vortex mixing (B); and vortex mixing plus a centrifugation step (C) for improved solution recovery. GFAP was subsequently determined using a commercial ELISA with optical detection. As shown in Fig. 2B, all protocols yielded a linear behavior when plotting measured vs. added GFAP ($R^2 > 0.99$, calculated as described in Methods section). However, recovery efficiencies differed substantially. Manual mixing showed the lowest recovery (64 ± 5%), whereas vortex mixing increased recovery to 88 ± 1%. The combination of vortex and centrifugation provided the highest recovery (99 ± 1%). In terms of volumetric recovery, the method

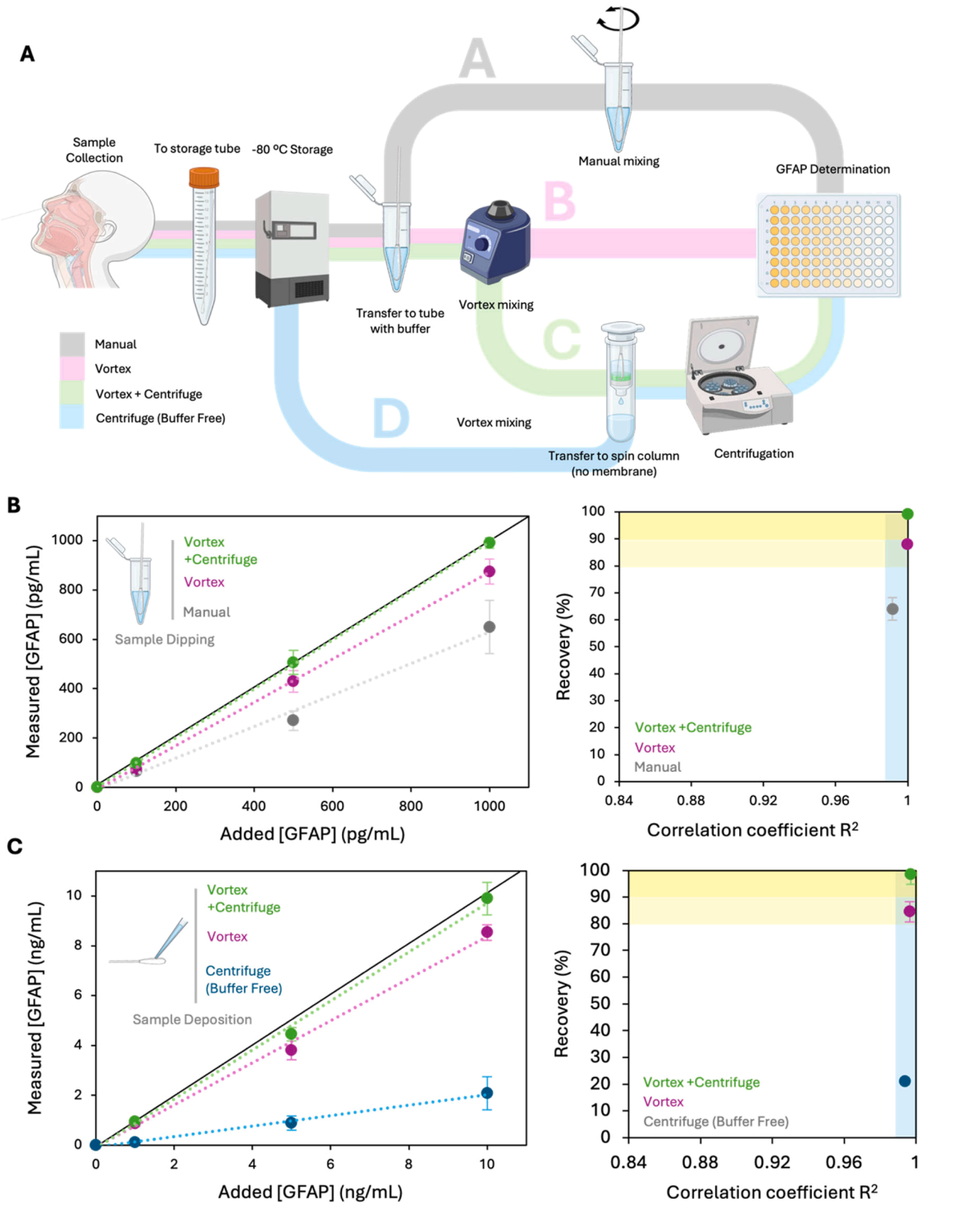



**Fig. 2.** Study for sample collection and recovery of flocked nylon swabs. A: Workflow for the four methodologies proposed. B and C: Protein recovery assay for a simulated sample (a GFAP solution in 10 mM PBS pH 7.4 containing 1% BSA) by dipping the swab (B) or depositing the simulated sample into the swab (C). Left: Results of measured vs. expected [GFAP]. Error bars indicate the SD of three devices. Black line represents 100% recovery. Right: Comparison of the recovery (%, slope) and the correlation coefficient ($R^2$). Dark and light-yellow boxes indicate excellent (>90%) and good (>80%) recoveries, respectively. Blue box represents linear behavior in terms of correlation coefficient ($R^2 > 0.99$). Error bars indicate the SD of the recovery *via* its linear estimation.

including the centrifugation protocol retrieved 95 ± 3% of the total liquid, indicating that almost all sample fluid was extracted from the device.

To replicate the experiment under more realistic sample-collection conditions, 12 μL of each simulated sample were deposited onto the swabs, and three of the protocols shown in Fig. 2A (see Methods section) were evaluated: vortex extraction (B), vortex extraction followed by centrifugation (C), and direct centrifugation without buffer (D). In this case, concentrations of the simulated samples were increased to the ng/mL range (1–10 ng/mL) to ensure operation within the linear range of the immunoassay. This modification was necessary because the amount of solution collected by the devices in the previous experiment was substantially higher, resulting in correspondingly higher concentrations in the recovery buffer. Manual mixing (A) was excluded from this experiment due to its lower recovery in the previous study. Instead, a buffer-free centrifugation protocol was incorporated to avoid sample dilution, allowing the collected material to be processed directly without the initial addition of 200 μL of recovery buffer. This approach reflects a more realistic downstream workflow in which minimizing dilution is advantageous for low-abundance biomarkers such as GFAP.

Results from this assay are shown in Fig. 2C, where, as in the previous experiment, all methods presented linear behavior ($R^2 > 0.99$). The vortex-based methods showed recovery values very similar to those obtained in the dipping assay, with recoveries of 85 ± 4% vs. 88 ± 1% for vortex extraction, and 98 ± 4% vs.99 ± 1% for the protocol including a centrifugation step. This consistency indicates that these sample processing methods are robust regardless of the sample loading procedure. In contrast, the buffer-free protocol yielded a markedly low recovery (21 ± 1%) confirming that the absence of a recovery buffer severely limits protein release from the device.

Furthermore, the volumetric recoveries of the buffer-free centrifugation vs. the vortex plus centrifugation protocol showed significant differences when comparing them (99 ± 2% and 97 ± 2%, respectively, $p = 0.009$, $n = 10$). Taken together, these results show that although avoiding the use of a recovery buffer allows most of the sample's liquid component to be extracted, the target protein largely remains retained within the swab, leading to markedly reduced GFAP recovery.

Regarding the novel collection devices, a few adjustments were performed to the protocols to adapt them to the characteristics of the devices. For the GrooveSwab®, as in the case of the deposited-sample assay described above, concentrations of the simulated samples had to be increased as the average collected sample mass (Fig. 1D) is only 8 ± 4 mg. In contrast, for Nasosorption™, the recovery volume had to be increased as this device is larger and more absorbent, and 200 μL, used for the nylon swabs, did not fully cover the device and thereby would yield reduced recoveries. Optimization experiments (Fig. S3) indicated that a volume of 1 mL in 2 mL microcentrifuge tubes was necessary to ensure complete coverage and efficient extraction when the Nasosorption™ swab was used.

In the case of the GrooveSwab®, the simulated sample was collected by dipping the device into 1 mL of the sample. Four methodologies were tested for the recovery study (Fig. 3A): vortex extraction (B), vortex extraction followed by centrifugation (C), and buffer-free centrifugation (performed either with (D) or without prior freezing (E), see the Methods section for details). As shown in Fig. 3B, none of these approaches yielded recoveries above 80%. However, clear differences were observed between methodologies. Protocols involving the fewest processing steps lead to the highest recoveries and best linearity, with only two of the methods exhibiting linear behavior. This was particularly evident for the vortex-based protocol, which requires a single processing step and provided the most consistent performance.

When involving a centrifugation step, and thus a transfer of the sample from either the initial tube or the buffer tube to the spin column, a marked loss of protein and a reduction in linearity were observed for both the vortex plus centrifugation protocol and the buffer-free centrifugation (Fig. 3B, green and blue dataset). This behavior can be attributed to the very small volume, retained by surface tension. Although weaker interactions between the sample and the device material should, in principle, favor protein recovery, the minimal volume makes handling considerably more challenging, as a substantial fraction can be lost unless manipulation is performed with extreme care. This is furthermore supported by the volumetric recoveries of these protocols: 81 ± 8% for the vortex plus centrifugation and 89 ± 1% for the buffer-free centrifugation (See Table 1 for full results). These data confirm that part of the sample is lost in the process, with a significant difference between methods ($p = 0.012$), as the vortex plus centrifuge method requires additional manipulation of the sample.

Because the GrooveSwab® is composed of polypropylene, interactions between GFAP and the device surface may also contribute to the observed recovery losses [24–26]. However, this remains a plausible but unconfirmed hypothesis in the present study. Additional factors such as handling losses, surface-tension retention, or freeze-thaw effects may also contribute to the observed behavior. To explore the influence of frozen storage, we evaluated a fourth protocol in which the sample was transferred directly to a spin column and centrifuged without a freeze-thaw step. It can be observed that this protocol (Fig. 3B, orange dataset) leads to an increase in both linearity ($R^2$ 0.992 vs. 0.861) and protein recovery (47 ± 3% vs.22 ± 6%) when compared to the equivalent protocol including the freezing step at −80 °C (Fig. 3B, orange vs. blue dataset). Furthermore, the volumetric recovery study of this protocol (98 ± 1%) indicated an improvement when compared to the vortex plus centrifuge (81 ± 8%, $p = 7.6 \cdot 10^{-5}$) and the buffer-free centrifugation protocols (89 ± 1%, $p = 1.2 \cdot 10^{-12}$).

To determine whether GFAP losses could be attributed to adsorption by the processing consumables (i.e., microcentrifuge tubes, spin columns), an additional control experiment was performed using the tubes and spin columns in the absence of any collection device. Four GFAP solutions with different concentrations (0, 1, 5 and 10 ng/mL) were prepared in the recovery buffer and either processed immediately or stored at −80 °C and thawed before being transferred through the spin columns under the same centrifugation conditions used in the device-processing protocols. Protein recoveries were 99.6 ± 0.6% ($R^2 = 0.99992$) and 99.4 ± 0.5% ($R^2 = 0.9998$) for immediately processed and frozen samples, respectively (Fig. S4), indicating that neither the processing consumables nor the freeze-thaw step alone caused measurable GFAP loss.

Taken together, these results indicate that the lower GFAP recovery observed after frozen storage of GrooveSwab® cannot be attributed to the tubes, spin columns, or the freeze-thaw step alone. Instead, the effect appears to depend on the collection device and/or the specific conditions under which the sample remains in contact with it. Prolonged contact with the GrooveSwab® polypropylene surface and surface-tension retention may contribute to the observed loss, although their individual effects cannot be distinguished from the present data. In addition, the higher recovery obtained with the single-step vortex protocol suggests that minimizing sample transfers and manipulation improves GFAP recovery when the GrooveSwab® is used.

In the case of Nasosorption™, the simulated sample was deposited onto the absorbent pad. As shown in Fig. 3C, all three evaluated methods (B, C, and D) resulted in poor linearity and protein recovery. As previously noted, the device does not become saturated during sample collection and can therefore absorb a substantial portion of the processing buffer. While this may facilitate liquid recovery, it also increases the likelihood that part of the sample remains unrecoverable within the device. This is further supported by the volumetric recovery obtained with the vortex plus centrifugation protocol, which was considerably lower than that of the flocked swab (88 ± 3% vs. 95 ± 3%). In contrast, volumetric recovery significantly improved when using the buffer free protocol (94 ± 3%, $p = 3.1 \cdot 10^{-4}$ (Nasosorption™ B vs. D; $n = 10$), indicating that a portion of the sample is indeed retained within the device. However, despite the improved volumetric recovery, protein recovery decreased under buffer-free conditions. We hypothesize that

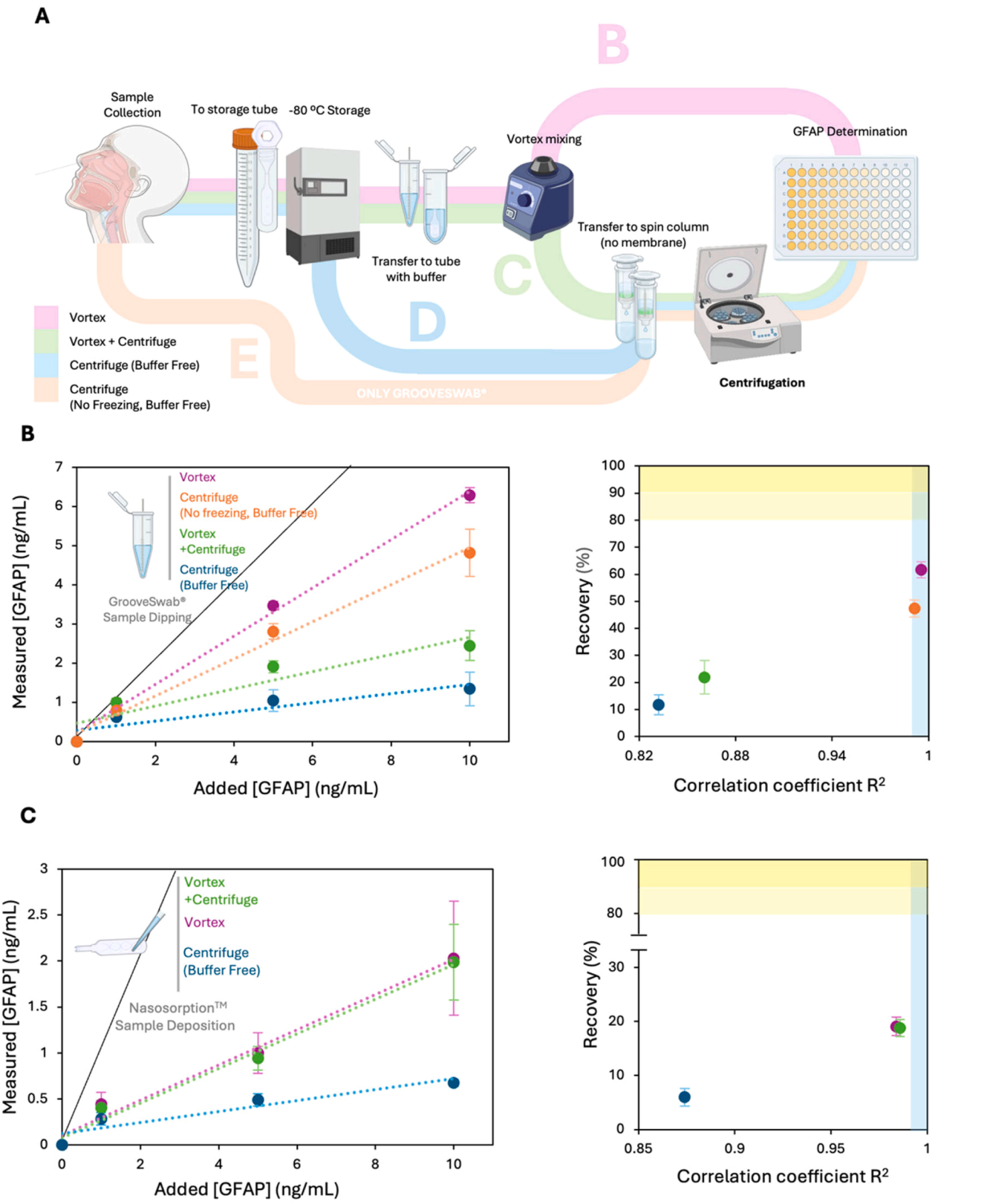



**Fig. 3.** Study for sample collection and recovery of GrooveSwab® and Nasosorption™ swabs. A: Workflow for the four methodologies proposed. B and C: Protein recovery assay for a simulated sample (GFAP solution in 10 mM PBS pH 7.4 containing 1% BSA) by dipping the GrooveSwab® (B) or depositing the sample onto the Nasosorption™ (C). Left: Results of measured vs. added [GFAP]. Error bars indicate the SD of the mean for three devices. Dark grey line represents 100% recovery. Right: Comparison of the recovery (%, slope) and the correlation coefficient ($R^2$). Dark and light-yellow boxes indicate both excellent (>90%) and good (>80%) recoveries, respectively. Blue box represents linear behavior in terms of correlation coefficient ($R^2$>0.99). Error bars indicate the SD of the recovery *via* its linear estimation.

**Table 1**
Summary of protein and volumetric recovery obtained for the three nasal-exudate collection devices using the evaluated processing protocols. Protein recovery was calculated from the slope of the linear regression between the expected and measured GFAP concentration for each device-protocol combination. Volumetric recovery was calculated gravimetrically and only for protocols involving centrifugation, in which the device was completely removed from the recovered solution (n = 10).

| Protein Recovery (%) | | | | |
|---|---|---|---|---|
| Device Protocol | Flocked nylon swab | | GrooveSwab® | Nasosorption™ |
| | Dipped | Deposited | Dipped | Deposited |
| Manual | 64 ± 5 | | | |
| Vortex | 88 ± 1 | 85 ± 4 | 62 ± 3 | 20 ± 2 |
| Vortex + Centrifuge | 99 ± 1 | 98 ± 4 | 22 ± 7 | 19 ± 2 |
| Centrifuge (buffer-free) | | 21 ± 1 | 12 ± 4 | 6 ± 2 |
| Centrifuge (no freezing, buffer-free) | | | 47 ± 3 | |
| **Volumetric recovery (%)** | | | | |
| Device Protocol | Flocked nylon swab | | GrooveSwab® | Nasosorption™ |
| | Dipped | Deposited | Dipped | Deposited |
| Vortex + Centrifuge | 95 ± 3 | 97 ± 2 | 81 ± 8 | 88 ± 3 |
| Centrifuge (buffer-free) | | 99 ± 2 | 89 ± 1 | 94 ± 3 |
| Centrifuge (no freezing, buffer-free) | | | 98 ± 2 | |

this effect is related to the structural characteristics of the SAM™, which appears under SEM microscopy to have a tightly woven-like structure, denser than that of the flocked swab. Cotton-based swabs have previously been reported to yield lower recoveries than nylon flocked fibers [22,27] and this limitation is likely exacerbated when working with low protein concentrations. Therefore, the protocols here proposed might be suitable for analytes at high concentration [28,29], as well as viral particles or bacteria, as previously reported, but not for the determination of low-abundance proteins.

Overall, the protein and volumetric recoveries obtained for the three collection devices using the different processing protocols are summarized in Table 1.

*Real sample analysis and further possibilities*

As a preliminary proof-of-concept assessment in clinical samples, nasal exudate from four stroke patients was collected using the three devices. Each sample was analyzed using the protocol with the highest recovery and linearity for its respective device: vortex plus centrifuge (C) for flocked nylon swabs, and vortex alone (B) for both GrooveSwab® and Nasosorption™. The results of this analysis are presented in Fig. 4A. As observed, flocked nylon swabs and the GrooveSwab® yielded concordant GFAP concentrations across patient samples. In the case of the Nasosorption™ swab, only one of the samples presented a concentration over the limit of detection of the method, and even in that case the measured concentration was markedly lower than those obtained with the other devices. These preliminary observations were consistent with the trends observed in the simulated-sample experiments.

However, it should be noted that these innovative devices were originally designed for the collection of infectious and respiratory samples, and therefore their use in this context falls outside their intended purpose. In the case of the GrooveSwab®, it allows sample extraction from the device without the need for a buffer solution, thereby avoiding dilution. Based on this feature, we propose a simple flick-based recovery protocol (Fig. 4B) in which the simulated sample (here, a 0.001% MB solution in 10 mM PBS) can be recovered by inserting the device into an empty tube and flicking it vigorously. As shown in the picture, the sample is released as a droplet in the bottom of the tube.

Although the Nasosorption™ swab showed limited recovery for low-abundance proteins such as GFAP, its flat geometry enables alternative workflows in which the device can be directly incorporated into paper-based microfluidic platforms. To illustrate this potential use case, we explored its integration into a lateral flow immunoassay as a proof-of-concept demonstration. In this approach, the device itself acts as the sample-collection element and is subsequently placed directly onto the sample-pad region of the LFIA, requiring only the addition of running buffer. This simplifies the workflow by eliminating the need for a separate extraction step. Nasosorption™ devices were spiked with 20 μL of SARS-CoV-2 positive or negative samples, and left to dry at room temperature for 5 min. Then, they were inserted into LFIA cassettes and 4 drops of the running buffer provided by the manufacturer were added. As shown in Fig. 4C, the resulting test lines matched the corresponding qPCR results. This experiment highlights an alternative and interesting functional role for Nasosorption™, demonstrating that beyond sample collection, the device can serve as an integrated component within paper-based microfluidic systems, potentially enabling workflows for liquid, dried, or low-volume samples.

## Discussion

This study critically evaluates three nasal exudate collection devices, flocked nylon swabs, GrooveSwab®, and Nasosorption™, focusing on their efficacy in collecting and recovering GFAP in nasal exudate for non-invasive point-of-care neurological diagnostics. Overall, flocked nylon swabs consistently outperformed the other devices across protocols, whereas GrooveSwab® and Nasosorption™ swabs showed limited efficiency for GFAP recovery. It is important to note that the matrix used in this work represents a simulated nasal exudate rather than the native biological matrix. This simplified model was intentionally selected to isolate device-dependent effects under controlled and reproducible conditions. Consequently, matrix-dependent effects associated with native NE were not directly assessed, and recovery values obtained using the PBS/BSA model should be interpreted as comparative rather than absolute recovery estimates for native NE.

The flocked nylon swabs proved to be the most effective for protein recovery across various protocols, especially when vortexing and centrifugation were applied. Their brush-like structure, composed of thousands of perpendicular nylon fibers, facilitates capillary uptake while maintaining open channels that promote efficient elution of the protein. This, combined with a flexible shaft that improves patient comfort, make this device well suited for NE sampling and GFAP recovery.

In contrast, GrooveSwab® and Nasosorption™ devices were less effective regarding protein recovery. For GrooveSwab®, the surface-tension-based collection mechanism and the small volumes collected likely contribute to incomplete elution and increased susceptibility to handling losses, which can be further hindered by sample loss during multi-step protocols. Nonetheless, it may be useful for high-protein samples in simplified protocols, as it can recover the entire sample volume without any dilution.

Nasosorption™ also showed limited GFAP recovery. The porous, capillary-driven fiber structure likely trapped the protein, reducing both protein and sample volume recovery. Although these limitations hold back its application for the analysis of proteins present at low concentrations, it has potential for use in the diagnosis of infectious diseases, where the target analytes are present in higher concentrations, as evidenced by its successful integration into lateral flow assays for SARS-CoV-2 detection.

Different recovery protocols were also assessed for each device in terms of volumetric recovery, with buffer-free centrifugation yielding higher volumetric recovery, likely because the workflow involves fewer handling steps and therefore minimizes sample loss. However, the

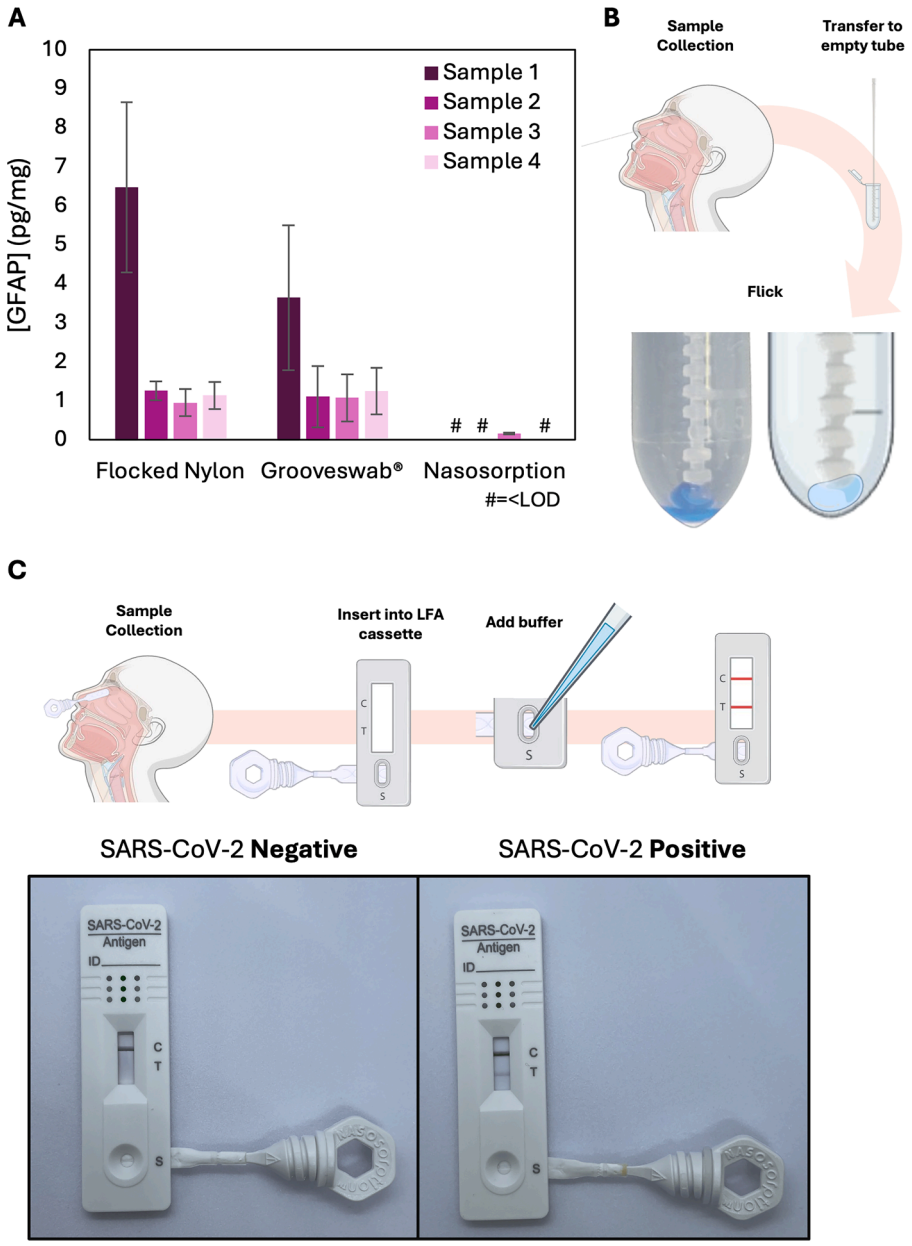



**Fig. 4.** Sample assessment using the three devices, and further possibilities of the GrooveSwab® and Nasosorption™ devices. A: Sample assessment of the devices using the protocols with the best recovery results. Error bars indicate the SD of three measurements. B: Proposed protocol for a simple one-step extraction, without dilution, of samples collected with the GrooveSwab®. Diagram on the right depicts the expected behavior of the protocol. Image on the left depicts a 0.001% solution of MB collected and recovered by flicking. C: Integrated use of the Nasosorption™ swab into lateral flow assays. The pictures show one negative and one positive sample, deposited into the device, for further assay by LFA.

absence of a recovery buffer resulted in lower protein yields, suggesting that GFAP remains partially retained within the device. This contrast highlights the trade-off between minimizing manipulation to preserve volume and ensuring efficient protein release from the collection material. For example, in the case of GrooveSwab®, immediate processing resulted in higher GFAP recovery than processing after frozen storage. Additionally, the control experiment without a collection device showed recoveries above 99% after both immediate processing and storage at −80 °C (Fig. S4). Thus, a single freeze-thaw cycle did not measurably reduce GFAP recovery in the recovery buffer under the tested conditions. The difference observed for GrooveSwab® therefore appears to be device-dependent and cannot be explained by the freeze-thaw step or adsorption to the processing consumables alone. Prolonged contact with the GrooveSwab® surface, device geometry, surface-tension retention, and sample handling may contribute to the observed loss, although the precise mechanism cannot be established from this study.

The differences observed between devices can be better understood by considering their distinct geometries, collection mechanisms, and material properties. Flocked nylon swabs maximize surface area while maintaining open channels for elution, supporting high GFAP recovery. GrooveSwab® retains small fluid volumes between polypropylene discs by surface tension, making sample handling and recovery challenging, while Nasosorption™ captures fluid by capillarity within a dense porous structure.

The preliminary analysis of nasal-exudate samples from four stroke patients showed trends consistent with those observed in the simulated-sample experiments, with flocked nylon swabs providing detectable GFAP measurements across all evaluated samples. However, the limited

number of patients (n = 4) is insufficient for clinical validation, and these results should be considered only as a preliminary proof-of-concept of the applicability of the sampling workflow.

In conclusion, the flocked nylon swab currently represents the most promising of the evaluated devices for GFAP determination from nasal exudate. GrooveSwab® and Nasosorption™ swabs, with very innovative designs, hold great potential with further refinement or for other diagnostic applications. These findings could guide the development of decentralized, rapid, and minimally invasive nasal-sampling workflows for GFAP analysis in the context of acute stroke triage.

## CRediT authorship contribution statement

**Pablo Rioboó-Legaspi:** Writing – original draft, Visualization, Methodology, Investigation, Formal analysis, Conceptualization. **Estefanía Costa-Rama:** Writing – review & editing, Supervision, Project administration, Methodology, Funding acquisition, Conceptualization. **Beatriz Fernández:** Writing – review & editing, Methodology. **Carmen García-Cabo:** Writing – review & editing, Resources, Methodology, Investigation. **Lorena Fernández-Benavente:** Writing – review & editing, Resources, Methodology. **Sergio Calleja-Puerta:** Writing – review & editing, Resources, Methodology. **M. Teresa Fernández-Abedul:** Writing – review & editing, Supervision, Project administration, Methodology, Funding acquisition, Conceptualization.

## Declaration of competing interest

The authors declare no competing interests.

## Acknowledgements

This work was supported by the I+D+i projects PID2020-118376RA-I00 and PID2023-148375OB-I00, (funded by MCIN/AEI/10.13039/501100011033, FEDER, EU) and IDE/2024/000694 funded by the Government of the Principality of Asturias and FEDER Program of the European Union through SEKUENS Agency. E.C.-R. was supported by the Spanish Ministry of Universities “Beatriz Galindo” grant (BG20/00027) and P.R.-L. by the Asturian Council for Science, Technology, and Innovation “Severo Ochoa” grant (BP21-029). Authors would like to thank Rhinostics Inc. for providing GrooveSwab® devices and, also, to Servicios Científico-Técnicos of the University of Oviedo for the technical support.

## Supplementary materials

Supplementary material associated with this article can be found, in the online version, at doi:10.1016/j.sampre.2026.100249.

## Data availability

The data that support the findings of this study, including the ESI, are available at the Repository of the University of Oviedo at the URL: https://hdl.handle.net/10651/85828 with the DOI: https://10.0.69.147/ruo_datasets.85828.

## References

[1] K. Fassbender, F. Merzou, M. Lesmeister, S. Walter, I.Q. Grunwald, A. Ragoschke-Schumm, et al., Impact of mobile stroke units cerebrovascular disease, J. Neurol. Neurosurg. Psychiatry 92 (2021) 815–822, https://doi.org/10.1136/jnnp-2020-324005.

[2] D. Karimova, E. Rostami, V.N. Chubarev, V.V. Tarasov, H.B Schiöth, M. Rask-Andersen, Advances in development of biomarkers for brain damage and ischemia, Mol. Biol. Rep. 51 (2024) 803, https://doi.org/10.1007/s11033-024-09708-x.

[3] V.K. Sharma, T.G. Singh, V. Mehta, A. Mannan, Biomarkers: role and scope in neurological disorders, Neurochem. Res. 48 (2023) 2029–2058, https://doi.org/10.1007/S11064-023-03873-4.

[4] O.S. Mattila, N.J. Ashton, K. Blennow, H. Zetterberg, H. Harve-Rytsälä, S. Pihlasviita, et al., Ultra-early differential diagnosis of acute cerebral ischemia and hemorrhagic stroke by measuring the prehospital release rate of GFAP, Clin. Chem. 67 (2021) 1361–1372, https://doi.org/10.1093/CLINCHEM/HVAB128.

[5] H.S. Jæger, D. Tranberg, K. Larsen, J.B. Valentin, R.A. Blauenfeldt, S. Luger, et al., Diagnostic performance of glial fibrillary acidic protein and prehospital stroke scale for identification of stroke and stroke subtypes in an unselected patient cohort with symptom onset < 4.5 h, Scand. J. Trauma Resusc. Emerg. Med. 31 (2023) 1–11, https://doi.org/10.1186/S13049-022-01065-7.

[6] A.H. Katsanos, K. Makris, D. Stefani, K. Koniari, E. Gialouri, M. Lelekis, et al., Plasma glial fibrillary acidic protein in the differential diagnosis of intracerebral hemorrhage, Stroke 48 (2017) 2586–2588, https://doi.org/10.1161/STROKEAHA.117.018409.

[7] B. Arslan, U. Andreasson, E. Rembeza, M. Axelsson, L. Novakova, B.E Kirsebom, et al., Validation of a plasma GFAP immunoassay and establishment of age-related reference values: bridging analytical performance and routine implementation, Clin. Chem. Lab. Med. 63 (2025) 2522–2535, https://doi.org/10.1515/CCLM-2025-0870.

[8] J. Chae, M. Choi, J. Choi, S.J. Yoo, The nasal lymphatic route of CSF outflow: implications for neurodegenerative disease diagnosis and monitoring, Anim. Cells Syst. 28 (2024) 45–54, https://doi.org/10.1080/19768354.2024.2307559.

[9] S.-J. Yoo, G. Son, J. Bae, S.Y. Kim, Y.K. Yoo, D. Park, et al., Longitudinal profiling of oligomeric aβ in human nasal discharge reflecting cognitive decline in probable Alzheimer's disease, Sci. Rep. 10 (2020) 11234, https://doi.org/10.1038/s41598-020-68148-2.

[10] Y.H. Kim, S.-M. Lee, S. Cho, J.-H. Kang, Y.-K. Minn, H. Park, et al., Amyloid beta in nasal secretions may be a potential biomarker of Alzheimer's disease, Sci. Rep. 9 (2019) 4966, https://doi.org/10.1038/s41598-019-41429-1.

[11] C. García-Cabo, P. Llano-Suárez, L. Benavente-Fernández, S. Calleja-Puerta, J. M. Costa-Fernández, M.T. Fernández-Abedul, Obtaining information from the brain in a non-invasive way: determination of iron in nasal exudate to differentiate hemorrhagic and ischemic strokes, Clin. Chem. Lab. Med. (CCLM) 58 (2020) 847–853, https://doi.org/10.1515/cclm-2019-0899.

[12] C. García-Cabo, P. Llano-Suárez, L. Benavente Fernández, J.M Costa-Fernández, M. T Fernández-Abedul, S. Calleja-Puerta, Iron measured in nasal exudate samples as a new and useful biomarker in the differential diagnosis of patients with acute stroke, Cerebrovasc. Dis. 49 (2020) 625–631, https://doi.org/10.1159/000511395.

[13] C. García-Cabo, P. Rioboó-Legaspi, L. Benavente-Fernández, E. Costa-Rama, M. T Fernández-Abedul, S. Calleja-Puerta, Measurement of GFAP in nasal exudate in the differential diagnosis between ischemic stroke and intracerebral hemorrhage, Cerebrovasc. Dis. 53 (2023) 515–518, https://doi.org/10.1159/000534693.

[14] M. Marina-Latorre, L. Lobo, C. García-Cabo, L. Benavente-Fernández, S. Calleja-Puerta, M. Teresa Fernández-Abedul, et al., Nasal exudate for diagnosis of stroke: fundamental studies through iron fractionation, total iron, and targeted protein determinations, Anal. Bioanal. Chem. 416 (2024) 5365–5375, https://doi.org/10.1007/s00216-024-05469-5.

[15] N. Hou, K. Wang, H. Zhang, M. Bai, H. Chen, W. Song, et al., Comparison of detection rate of 16 sampling methods for respiratory viruses: a bayesian network meta-analysis of clinical data and systematic review, BMJ Glob. Health 5 (2020) e003053, https://doi.org/10.1136/bmjgh-2020-003053.

[16] G. Guido, M.N. Losio, G. Varisco, FLOQSwab™: optimisation of procedures for the recovery of microbiological samples from surfaces, Ital. J. Food Saf. 5 (2016) 121–123, https://doi.org/10.4081/IJFS.2016.5756.

[17] N.M. Wise, S.J. Wagner, T.J Worst, J.E. Sprague, C.M. Oechsle, Comparison of swab types for collection and analysis of microorganisms, Microbiologyopen 10 (2021), https://doi.org/10.1002/mbo3.1244.

[18] R.S. Thwaites, H.C. Jarvis, N. Singh, A. Jha, A. Pritchard, H. Fan, et al., Absorption of nasal and bronchial fluids: precision sampling of the human respiratory mucosa and laboratory processing of samples, J. Vis. Exp. (2018), https://doi.org/10.3791/56413.

[19] J. Hedman, Y. Akel, L. Jansson, R. Hedell, N. Wallmark, C. Forsberg, et al., Enhanced forensic DNA recovery with appropriate swabs and optimized swabbing technique, Forensic Sci. Int. Genet. 53 (2021) 102491, https://doi.org/10.1016/j.fsigen.2021.102491.

[20] B.B. Bruijns, R.M. Tiggelaar, H. Gardeniers, The extraction and recovery efficiency of pure DNA for different types of swabs, J. Forensic Sci. 63 (2018) 1492–1499, https://doi.org/10.1111/1556-4029.13837.

[21] C. Rock, M. Anderson, S. Lewis, V. Scheeler, E. Nowakowski, Y.-J. Hsu, et al., Comparison of nylon-flocked swab and cellulose sponge methods for carbapenem-resistant Enterobacteriaceae and gram-negative organism recovery from high-touch surfaces in patient rooms, Infect. Control Hosp. Epidemiol. 39 (2018) 1257–1261, https://doi.org/10.1017/ice.2018.182.

[22] A. Probst, R. Facius, R. Wirth, C. Moissl-Eichinger, Validation of a nylon-flocked-swab protocol for efficient recovery of bacterial spores from smooth and rough surfaces, Appl. Environ. Microbiol. 76 (2010) 5148–5158, https://doi.org/10.1128/AEM.00399-10.

[23] L. Jansson, Y. Akel, R. Eriksson, M. Lavander, J. Hedman, Impact of swab material on microbial surface sampling, J. Microbiol. Methods 176 (2020) 106006, https://doi.org/10.1016/j.mimet.2020.106006.

[24] O.A Kofanova, K. Mommaerts, F. Betsou, Tube polypropylene: a neglected critical parameter for protein adsorption during biospecimen storage, Biopreservation Biobanking 13 (2015) 296–298, https://doi.org/10.1089/BIO.2014.0082.

[25] M. Schvartz, F. Saudrais, S. Devineau, J.C. Aude, S. Chédin, C. Henry, et al., A proteome scale study reveals how plastic surfaces and agitation promote protein

aggregation, Sci. Rep. 13 (2023) 1–17, https://doi.org/10.1038/s41598-023-28412-7.
[26] P.E Bratcher, A. Gaggar, Characterization and prevention of the adsorption of surfactant protein D to polypropylene, PLoS One 8 (2013) e73467, https://doi.org/10.1371/JOURNAL.PONE.0073467.
[27] A. Gray, A. Kuffel, N.N. Daeid, An improved rapid method for DNA recovery from cotton swabs, Forensic Sci. Int. Genet. 64 (2023) 102848, https://doi.org/10.1016/j.fsigen.2023.102848.
[28] H. Owles, J. Baker, P. Fenwick, S. Elkin, K. Kasmi, P. Barnes, et al., S28Non-invasive nasal sampling using nasosorption may identify COPD inflammatory profiles and have a role as a diagnostic tool in exacerbations, Thorax 78 (2023) A24, https://doi.org/10.1136/thorax-2023-BTSabstracts.34.
[29] R.S. Thwaites, K. Ito, J.M.S. Chingono, M. Coates, H.C. Jarvis, T. Tunstall, et al., Nasosorption as a minimally invasive sampling procedure: mucosal viral load and inflammation in primary RSV bronchiolitis, J. Infect. Dis. 215 (2017) 1240–1244, https://doi.org/10.1093/infdis/jix150.